Communication

Multiplexed Multicolor Raman Imaging of Live Cells with Isotopically Modified Single Walled Carbon Nanotubes

Zhuang Liu, Xiaolin Li, Scott M. Tabakman, Kaili Jiang, Shoushan Fan, and Hongjie Dai

J. Am. Chem. Soc., **2008**, 130 (41), 13540-13541 • DOI: 10.1021/ja806242t • Publication Date (Web): 20 September 2008

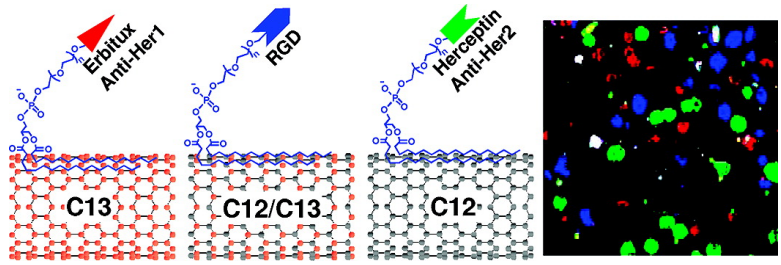

More About This Article

Additional resources and features associated with this article are available within the HTML version:

- Supporting Information
- Access to high resolution figures
- Links to articles and content related to this article
- Copyright permission to reproduce figures and/or text from this article

View the Full Text HTML

J|A|C|S
COMMUNICATIONS

Published on Web 09/20/2008

Multiplexed Multicolor Raman Imaging of Live Cells with Isotopically Modified Single Walled Carbon Nanotubes

Zhuang Liu,[†] Xiaolin Li,[†] Scott M. Tabakman,[†] Kaili Jiang,[‡] Shoushan Fan,[‡] and Hongjie Dai*,[†]

Department of Chemistry, Stanford University, Stanford, California 94305, and Department of Physics and Tsinghua-Foxconn Nanotechnology Research Center, Tsinghua University, China

Received August 7, 2008; E-mail: hdai@stanford.edu

Fluorescence techniques have been widely used in biological imaging, though nonideal factors exist including photobleaching of organic dyes, autofluorescence background from biological tissues, and wide fluorescence excitation and emission peaks giving rise to spectra overlays that limit the use of multiple colors in an experiment.[1] Raman scattering has narrow spectral lines that could be used for imaging with high multiplicity. In addition, tissue autofluorescence problems could be circumvented since sharp Raman peaks could be differentiated from fluorescence background. Raman excitation can also be chosen in low-background and biologically transparent optical windows. Raman imaging is promising for the next generation of biological imaging.[2−4]

Single walled carbon nanotubes (SWNTs)[2,5−13] and other nanomaterials[14,15] have been explored in biological and medical areas including drug delivery and imaging. As one-dimensional quantum wires with a sharp electronic density of states at the van Hove singularities, SWNTs exhibit intrinsic optical properties including photoluminance in the NIR range[5,10] and strong resonant Raman scattering,[6,7] both of which have been used for biological imaging. Single-color SWNT Raman imaging of biological specimens has been studied previously,[2,6,7] but multicolor Raman imaging with SWNTs remains unexplored. Here, we show that SWNTs with different isotope compositions display well-shifted Raman G-band peaks[16,17] and can serve as different colors for Raman imaging. Cancer cells with specific receptors are selectively tagged with three different "color" SWNTs, allowing for multicolor Raman imaging of cells in a multiplexed manner.

Pure C12-SWNTs (C12-SWNT) were obtained commercially, while pure C13 SWNTs (C13-SWNT) and C12/C13 mixed SWNTs (C12/C13-SWNT) were synthesized by chemical vapor deposition (CVD) as previously reported[18] using C13-methane and mixed C12/C13 methane, respectively. Note that CVD is a scalable and economic method for the synthesis of nanotubes, even with C13-methane. Phospholipid-PEG-amine (DSEP-PEG5000-Amine) functionalized C12-SWNT, C13-SWNT, and C12/C13-SWNTs were conjugated to Herceptin (anti-Her2), Erbitux (anti-Her1), and arginine-glycine-aspartic acid (RGD) peptide to recognize Her2/neu, Her1/EGFR, and integrin $\alpha_v\beta_3$ cell-surface receptors, respectively (Figure 1a), following established protocols.[5,9] We chose these ligand−protein systems due to their importance in cancer biology and medicine. The Her1/EGFR and Her2/neu receptors belong to the ErbB protein family and are overexpressed on various cancer cells especially breast cancer cells.[19] Integrin $\alpha_v\beta_3$ is a cell surface receptor related to cancer angiogenesis and metastasis and is up-regulated on various solid tumor cells and fast growing tumor vasculatures.[20]

Raman spectra of C12, C12/C13, and C13 SWNT conjugates were recorded under a near-infrared (NIR) 785 nm laser excitation,

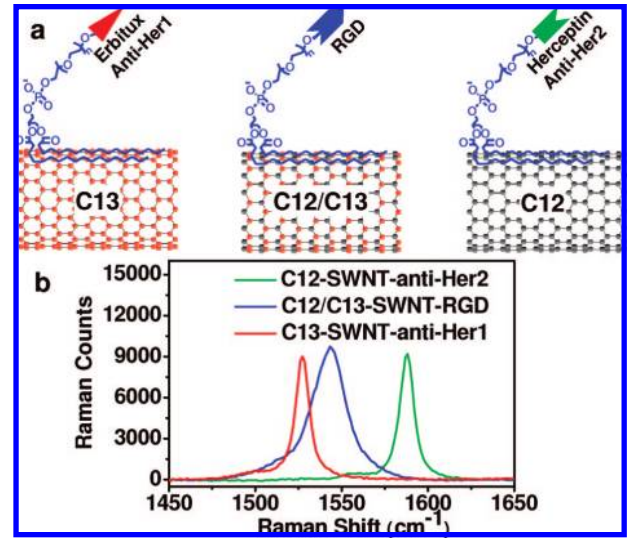

Figure 1. SWNTs with different Raman colors. (a) Schematic SWNTs with three different isotope compositions (C13-SWNT, C12/C13-SWNT, C12-SWNT) conjugated with different targeting ligands. (b) Solution phase Raman spectra of the three SWNT conjugates under 785 nm laser excitation. Different G-band peak positions were observed. At the same SWNT concentration, the peak height of C12-SWNT (Hipco) was ∼2 times higher than that of C13-SWNT and ∼4 times higher than that of C12/C13-SWNT. For mixtures used in biological experiments, concentrations of the three SWNTs were adjusted to give similar G-band peak intensities of the three colors, as shown in this figure.

displaying well-shifted Raman G-band peaks at 1590, 1544, and 1528 cm^{-1} (Figure 1b), as expected from the isotope effect.[16,17] We first incubated BT474 breast cancer cells (Her2+) with C12-SWNT-anti-Her2 for 2 h at 4 °C (to prevent endocytosis of nanotubes).[21] The cells were imaged by a confocal Raman microscope after washing with phosphate buffered saline (PBS) 3 times to remove nonspecifically bound nanotubes on cells. Live cells were used directly for imaging. With a 0.5 s collection time at each pixel, a full Raman spectroscopy image required 1−2 h. This time could be shortened to ∼20 min by using a higher power laser and adjusting the binning factor in the spectrometer. Association of SWNTs to the BT cells were clearly observed in high resolution confocal Raman spectroscopy images (Figure 2). The targeting specificity was evidenced by the low SWNT signal observed when cells were incubated with nanotubes without antibody conjugation (data not shown).

Next, we mixed the three-color ligand−SWNTs for multiplexed cell imaging. Concentrations of the three SWNTs in the mixture were adjusted to give similar G-band peak intensities of the three colors. The peak shift from C12-SWNT to C13-SWNT was large without overlapping and can be easily separated (SI Figure S1). The Raman spectrum of our three-color SWNT mixture (C12-

[†] Stanford University.
[‡] Tsinghua University.

10.1021/ja806242t CCC: $40.75

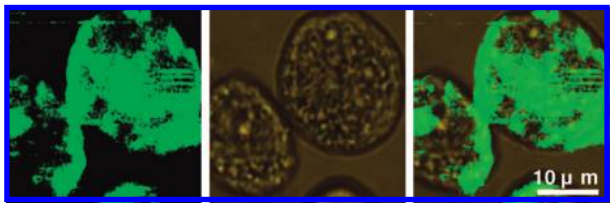

Figure 2. A confocal Raman spectroscopy image (left) of BT474 cells (optical image in middle, overlay image at right) after incubation with C12-SWNT-anti-Her2. Raman images were recorded with <1 μm spatial resolution (see SI).

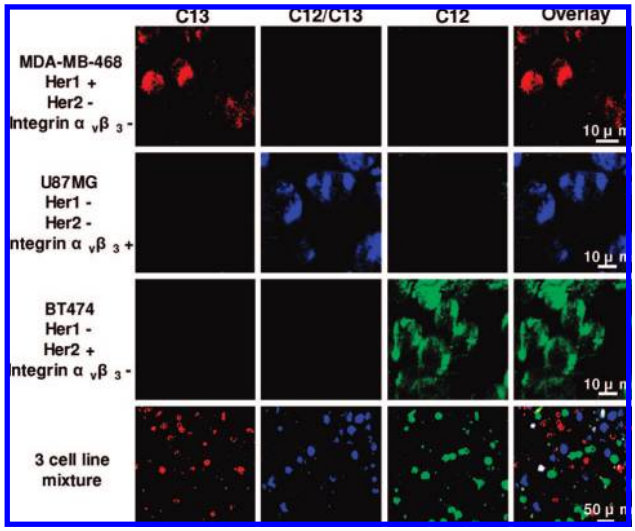

Figure 3. Multicolor Raman imaging with SWNTs. Deconvoluted confocal Raman spectroscopy images of three different cell lines after incubation with a mixture of the three-color SWNTs (top 3 rows, red, blue, green colors are Raman intensities of C12, C12/C13, and C13 SWNTs, respectively). In the bottom row, a mixture of three cell lines was incubated with the three-color SWNT mixture. Those images clearly show a mixture of cells with differentiated Raman labeling by three types of SWNTs. Occasional colocalization of different colors could due to dead cells or nonspecific nanotube binding.

SWNT-anti-Her2, C13-SWNT-anti-Her1, C12/C13-SWNT-RGD) however showed overlaps between adjacent peaks. Deconvolution of a recorded Raman spectrum into the spectra of the three SWNT samples was done to analyze the relative amounts of each color in any mixture and on live cells.

Three types of cells including BT474 (human breast cancer, Her2+), U87MG (human glioblastoma, Integrin $\alpha_v\beta_3$+), and MDA-MB-468 (human breast cancer, Her1+) were incubated with the three-color SWNT mixture and then subjected to confocal Raman spectroscopy imaging. After background subtraction, the Raman spectrum recorded at each location ("pixel") was deconvoluted to intensities of the three colors (C12, C12/C13, C13) at each pixel, which was used to create images of the three colors representing the Raman signals of the different SWNTs (see SI for details). The resulting Raman spectroscopy images of three cell lines showed specific labeling of cells by SWNTs with minimal nonspecific binding (Figure 3, top three rows; SI Figure S1). Furthermore, a mixture of the three cell lines was incubated with the three-color SWNT mixture. The Raman images clearly identified the existence of three cell types, each labeled by a distinct Raman color (Figure 3, bottom row). This demonstrated the ability of multiplexed cell identification/imaging by SWNTs with different isotope compositions, for probing and imaging of several biological species simultaneously.

More SWNT Raman colors have been obtained previously by varying C12/C13 ratios in SWNTs.[17] Since the peak difference between C13-SWNT and C12-SWNT is 62 cm^{-1} and that between C13-SWNT and C12/C13-SWNT is 16 cm^{-1}, more colors can be used for further multiplexing. The full width at half-maximum (fwhm) of the SWNT G peak is <2 nm, allowing for the SWNT Raman spectral features to be easily distinguished from the autofluorescence background of cells. With a laser excitation of 785 nm, the excitation and scattered photons are well within the NIR range (700−900 nm), which is in the most transparent optical window for biological imaging. Compared with other surface enhanced Raman scattering (SERS) nanoparticles,[2,4] SWNT Raman tags are simpler systems with well established synthesis methods.[18,22] The single isolated Raman G peak of SWNTs is also desirable. SWNTs exhibit high chemical inertness and stability, with robust Raman signals against photobleaching, which compares favorably over organic molecules.[7] This allows for tracking and imaging over long periods of time.[12] In addition to the isotope-dependent Raman colors, SWNTs with controlled diameters also exhibit distinctive Raman peaks in their radial-breathing modes,[23] which can also be used for multicolor Raman imaging. Lastly, the various SWNT Raman colors can easily be excited with a single light source. Taken together, SWNTs are promising new Raman tags for multiplexed detection and imaging for biological systems.

Acknowledgment. We thank Drs. Sanjiv Gamhhir, Dean Felsher, and Xiaoyuan Chen for providing us Herceptin, Erbitux, and RGD, respectively. This work was supported by NIH-NCI CCNE-TR, NIH-NCI R01 CA135109-01, and a Stanford graduate fellowship.

Supporting Information Available: Experimental details and other supplementary data.This material is available free of charge via the Internet at http://pubs.acs.org.

References

(1) Wagnieres, G. A.; Star, W. M.; Wilson, B. C. *Photochem. Photobiol.* **1998**, *68*, 603–632.
(2) Keren, S.; Zavaleta, C.; Cheng, Z.; de la Zerda, A.; Gheysens, O.; Gambhir, S. S. *Proc. Natl. Acad. Sci. U.S.A.* **2008**, *105*, 5844–5849.
(3) Baena, J. R.; Lendl, B. *Curr. Opin. Chem. Biol.* **2004**, *8*, 534–539.
(4) Qian, X. M.; Peng, X. H.; Ansari, D. O.; Yin-Goen, Q.; Chen, G. Z.; Shin, D. M.; Yang, L.; Young, A. N.; Wang, M. D.; Nie, S. M. *Nat. Biotechnol.* **2008**, *26*, 83–90.
(5) Welsher, K.; Liu, Z.; D, D.; Dai, H. *Nano Lett.* **2008**, *8*, 586–590.
(6) Liu, Z.; Winters, M.; Holodniy, M.; Dai, H. J. *Angew. Chem., Int. Ed.* **2007**, *46*, 2023–2027.
(7) Heller, D. A.; Baik, S.; Eurell, T. E.; Strano, M. S. *Adv. Mater.* **2005**, *17*, 2793–2799.
(8) Schipper, M. L.; Nakayama-Ratchford, N.; Davis, C. R.; Kam, N. W. S.; Chu, P.; Liu, Z.; Sun, X.; Dai, H.; Gambhir, S. S. *Nat. Nanotechnol.* **2008**, *3*, 216–221.
(9) Liu, Z.; Sun, X.; Nakayama, N.; Dai, H. *ACS Nano* **2007**, *1*, 50–56.
(10) Cherukuri, P.; Bachilo, S. M.; Litovsky, S. H.; Weisman, R. B. *J. Am. Chem. Soc.* **2004**, *126*, 15638–15639.
(11) Kam, N. W. S.; O'Connell, M.; Wisdom, J. A.; Dai, H. *Proc. Natl. Acad. Sci. U.S.A.* **2005**, *102*, 11600–11605.
(12) Liu, Z.; Davis, C.; Cai, W.; He, L.; Chen, X.; Dai, H. *Proc. Natl. Acad. Sci. U.S.A.* **2008**, *105*, 1410–1415.
(13) Liu, Z.; Cai, W. B.; He, L. N.; Nakayama, N.; Chen, K.; Sun, X. M.; Chen, X. Y.; Dai, H. J. *Nat. Nanotechnol.* **2007**, *2*, 47–52.
(14) Wang, L.; Zhao, W.; Tan, W. *Nano Res.* **2008**, *1*, 99–115.
(15) Sun, X.; Liu, Z.; Welsher, K.; Robinson, J. T.; Goodwin, A.; Zaric, S.; Dai, H. *Nano Res.* **2008**, *1*, 203–212.
(16) Liu, L.; Fan, S. S. *J. Am. Chem. Soc.* **2001**, *123*, 11502–11503.
(17) Rummeli, M. H.; Loffler, M.; Kramberger, C.; Simon, F.; Fulop, F.; Jost, O.; Schonfelder, R.; Gruneis, A.; Gemming, T.; Pompe, W.; Buchner, B.; Pichler, T. *J. Phys. Chem. C* **2007**, *111*, 4094–4098.
(18) Li, X. L.; Tu, X. M.; Zaric, S.; Welsher, K.; Seo, W. S.; Zhao, W.; Dai, H. J. *J. Am. Chem. Soc.* **2007**, *129*, 15770.
(19) Rowinsky, E. K. *Annu. Rev. Med.* **2004**, *55*, 433–457.
(20) Jin, H.; Varner, J. *Br. J. Cancer* **2004**, *90*, 561–565.
(21) Kam, N. W. S.; Liu, Z. A.; Dai, H. J. *Angew. Chem., Int. Ed.* **2006**, *45*, 577–581.
(22) Dai, H. *Acc. Chem. Res.* **2002**, *35*, 1035–1044.
(23) Rao, A. M.; Richter, E.; Bandow, S.; Chase, B.; Eklund, P. C.; Williams, K. A.; Fang, S.; Subbaswamy, K. R.; Menon, M.; Thess, A.; Smalley, R. E.; Dresselhaus, G.; Dresselhaus, M. S. *Science* **1997**, *275*, 187–191.

JA806242T